www.czasopisma.pan.pl www.journals.pan.pl

Arch. Metall. Mater. **68** (2023), 4, 1401-1410

DOI: https://doi.org/10.24425/amm.2023.146206

P. SINGH[1*], R.K. SINGH[2,3], A.K. DAS[1]

EFFECT OF DIFFERENT CERAMIC REINFORCEMENTS ON MICROSTRUCTURE, MECHANICAL PROPERTIES AND TRIBOLOGICAL BEHAVIOUR OF THE Al6082 ALLOY PRODUCED BY STIR CASTING PROCESS

In the present study, the mechanical properties and high-temperature sliding wear behaviour of the Al6082-SiC-TiO_2 hybrid composite in different environmental conditions produced by the stir-casting process were investigated and distinguished with single-reinforced composites (Al6082-SiC and Al6082-TiO_2) and matrix alloy. The microstructure of composites exhibited a reasonably uniform scatter of particles in the aluminium matrix with good bonding between the matrix-particle interfaces. The hybrid composite's hardness and ultimate tensile strength showed higher hardness and tensile strength than matrix alloy and single-reinforced composites, whereas trends were reversed for the elongation. The impact test of the materials was conducted at different temperatures (room temperature, 0°C, –25°C, –50°C, and –75°C). The hybrid composite shows higher impact strength than the other materials, and impact strength decreases with temperature because ductility decreases with temperature. The fracture surfaces were examined to identify the fracture mechanism. The sliding wear test was conducted at different temperatures (room temperature, 100°C, 175°C, 250°C and 325°C) to distinguish the tribological behaviour of materials. The weight loss of the materials was increased with an increase in temperatures. The hybrid composite shows a lower weight loss than the other condition samples, irrespective of the temperatures. The wear surfaces were examined to predict the material removal mechanism.

Keywords: Al6082 alloy; Low-temperature impact properties; SiC particles; TiO_2 particles; Hybrid Composites; High-temperature wear properties

1. Introduction

In the present scenario, manufacturing lightweight automotive vehicles is in high demand on a global scale. As a result, continuing research is being carried out to identify materials with adequate strength-to-weight ratios, such as aluminium alloys. Aluminium alloys are extensively used in numerous engineering fields, such as automotive, aerospace, military, and marine, owing to their exceptional qualities like outstanding corrosion resistance, low weight, and excellent stiffness [1-2]. However, poor wear behaviour is a negative aspect of aluminium alloys, and this aspect is solved by distributing reinforcements (like SiC, Al_2O_3, SiO_2, B_4C, TiB_2, ZrO_2, Si_3N_4 etc.) in aluminium alloys, also referred to as aluminium matrix composites (AMCs) [3-9]. AMCs are widely used in automotive and aeronautical industries because of their superior strength-to-weight ratio, good corrosion resistance, high wear resistance, favourable mechanical properties, higher thermal diffusivity, low thermal expansion, and higher thermal conductivity [10-11]. Aluminium hybrid matrix composites (AHMCs) are new-generation composites with more than one type of reinforcement with different shapes and sizes to gain better properties [12-16].

The literature reveals that the mechanical properties of AMCs were thoroughly investigated and well understood, but there needs to be more information available about these materials' toughness. However, these composites' toughness-impact strength has been studied in many research works at room temperature using various materials and processing parameters [17-22]. In contrast, very few studies on the behaviour of Al-SiC composites at different temperatures [23-24] and no studies were done on the Al-SiC-TiO_2 composites. For a temperature range of 25°C (room temperature) to –75°C, the Al-SiC-TiO_2 composites have significant applications in various industries; therefore impact behaviour of Al/SiC/TiO_2 composites needs to be investigated.

AMCs are a reliable alternative for aluminium alloys, cast iron, and steel to achieve energy savings, durability, and environmental-economic benefits. As a result, AMCs are employed

1 NATIONAL INSTITUTE OF TECHNOLOGY, DEPARTMENT OF MECHANICAL ENGINEERING, ASHOK RAJPATH, MAHENDRU, PATNA, BIHAR, 800005, INDIA
2 UNIVERSITY ROAD, DEPARTMENT OF MECHANICAL ENGINEERING, REWA ENGINEERING COLLEGE, REWA, MADHYA PRADESH, 486002, INDIA
3 VINDYA INSTITUTE OF TECHNOLOGY AND SCIENCE, MECHANICAL ENGINEERING, AMAUDHA KALAN, SATNA, MADHYA PRADESH, 485001, INDIA

* Corresponding author: pushprajs.phd18.me@nitp.ac.in

in many industrial and automotive parts where wear and tear, weight savings, and seizure are major issues. These items include driveshafts, cylinder heads, connecting rods, pistons, and brake drums for the automobile industry. The mining and maritime sectors include impellers, valves, and turbine blades [25-32]. Usually, those components have experienced different kinds of surface defects like wear and tear. Thus, there is a need to study the wear characterisation of AMCs under different conditions. Several investigations have focused on the abrasive wear and sliding behaviour of AMCs [33-45,3,7]. In contrast, very few studies have focused on the dry sliding wear behaviour of AMCs at high temperatures.

Against this background, the present work examined the microstructure, mechanical characteristics and material removal mechanism on the high-temperature sliding wear behaviour of the Al-SiC-TiO_2 composites and their base alloys. Additionally, the fracture surface and wear surfaces were also examined through a scanning electron microscope (SEM).

2. Materials and methods

2.1. Matrix material and reinforcements

Al6082 was selected as a metal matrix material for the present investigation. The optical emission spectrometer (SPECTROMAXx LMF05, SPECTRO, made in Germany) was used for verifying the chemical ingredients of Al6082 alloy, as shown in TABLE 1. The SiC and TiO_2 particles, with a mean size of 10 µm and 5 µm, respectively, were taken for the reinforcement.

TABLE 1

Chemical ingredients of Al6082 alloy

Element	Mg	Al	Si	Mn	Ti	Fe	Cu	Zn	Zr
%wt	1.00	97.38	1.08	0.34	0.04	0.06	0.08	0.02	0.00

2.2. Experimentation

The experiments were designed to compare Al6082 alloys, composites (SiC/TiO_2 as reinforcements) and hybrid composites shown in TABLE 2. The investigation was carried out by melting the Al6082 alloy ingot in an induction furnace and heated up to 760°C. The super-heated molten metal was taken into a ladle, stirring induced into molten metal using the 4-axial mechanical stirrer blade speed of 700 rpm. The preheated ceramic powders were introduced into molten metal while stirring, and molten metal was degassed using argon gas. Uniform distribution of ceramic powders was done by stirring for 10 minutes. The molten metal slurry was poured into a preheated hardened mild steel mould; subsequent solidification was carried out.

TABLE 2

Design of Experiments

Exp No.	Condition
E-1	Al6082 alloy
E-2	Al6082+3%SiC composite
E-3	Al6082+3% TiO_2 composite
E-4	Al6082+1.5%SiC+1.5%TiO_2 hybrid composite

2.3. Characterisation

2.3.1. Microstructural characterisation

Microstructural analysis of prepared samples was carried out using a scanning electron microscope (model-JEOL JSM-6480LV) outfitted with an Energy-Dispersive X-ray analyser (EDX). The samples were prepared with a dimension of 10 mm×10 mm. The samples were polished using different grades of emery paper (320, 600, 800, 1200, 1500, and 2000 grades), followed by velvet cloth polishing using diamond paste and ethanol. Keller's reagent was used as the etching reagent (1.5 ml HCl, 2.5 ml HNO_3, 1.0 ml HF, and 95 ml water).

2.3.2. XRD characterisation

An Ultima IV X-ray diffractometer with CuK alpha radiation and Nickel filter was used for phase analysis of different composites. 30 mA current intensity and a voltage of 40 kV, respectively, were the analysis parameters.

2.3.3. Mechanical properties

Tensile and impact samples were prepared using a wire-cutting machine (EDM). The tensile test specimens were prepared according to ASTM standards E8/E8M–04. Tensile tests were carried out by applying a universal hydraulic testing machine (Instron 8501) with a capacity of 125 kN, and the tests were conducted at a ram speed of 0.35 mm per min and an initial strain rate of 1.69×10^{-4} s^{-1}.

The Impact tests were performed using instrumented Charpy tester (model-Zwick GmbH) with a low-temperature capacity of up to –196°C. The impact tests were performed at different temperatures of (room temperature, 0°C, –25°C, –50°C, and –75°C). Impact test carried samples with V-notch was prepared as per ASTM E23-12C of dimensions 55 mm×10 mm×10 mm and kept in liquid nitrogen for 10 minutes before the tests. The time gap between the taking away of samples from the liquid nitrogen to the tests was at least 5 seconds according to the standard of ASTM E23. After the tensile and impact test, the fracture surfaces of the materials were investigated using Scanning Electron Microscopy (Model-JEOL JSM-6480LV).

The hardness tests were performed using the Brinell hardness testing machine. The testing load was 250N applied for 30 seconds, and the ball size of the indentor was 5 mm in diameter. A sample size of 20 mm × 20 mm was prepared for the hardness testing. An average of three indentations was taken for hardness value calculation in each sample.

2.3.4. Wear characterisation

The sliding wear tests of samples were conducted at different temperatures (RT, 100°C, 175°C, 250°C and 325°C) at loads 10 kN for a speed of 500 rpm. The sliding distance was fixed at 1200 m. A pin-on-disc sliding wear testing instrument (model: DUCOM-TR 20-LE) was used for the wear test, and a standard steel disc having a surface roughness of less than one micron was used. The wear samples (pins) size was 10 mm in diameter and 35 mm in length. The wear samples were dipped and appropriately cleaned before and after the test performance. For high-temperature wear tests, the pin-on-disc was surrounded by a hot chamber furnace to maintain a constant temperature. Three individual wear and friction tests were performed, and the mean value was taken. The rate of wear was calculated by the weight loss method. After the wear test, the wear surfaces of the materials were investigated using SEM (model-JEOL JSM-6480LV).

3. Results and discussion

3.1. Microstructural analysis

SEM images were taken for microstructural analysis, and EDX analysis was performed for elemental analysis of different materials (E-1, E-2, E-3, and E-4). Fig. 1(a) depicts the microstructure of E-1, and grain boundaries of α-Aluminum were encircled. Fig. 1(d) illustrates the EDX analysis of Al6082 alloy, confirming that all the major and minor elements present with appropriate weight %. Figs. 1(b and c) shows the morphology of reinforcement materials (SiC and TiO_2). The microstructure of composite samples was also examined using SEM. Fig. 2(a) represents the microstructure of E-2 and exhibits that the SiC particles (encircled) are distributed uniformly in the aluminium matrix. Fig. 2(b) shows the microstructure of E-3 and that the TiO_2 particles are distributed throughout the matrix. In contrast, Fig. 2(c) shows the microstructure of E-4 with a fine microstructure and clustering of particles. Fig. 2(d) shows the elemental analysis of hybrid composites through the EDX area mapping method, confirming the presence of SiC and TiO_2 particles and other elements with appropriate weight percentages throughout the matrix. The aluminium matrix can be seen as a dark region and reinforcements (SiC and TiO_2 particles) as grey and white

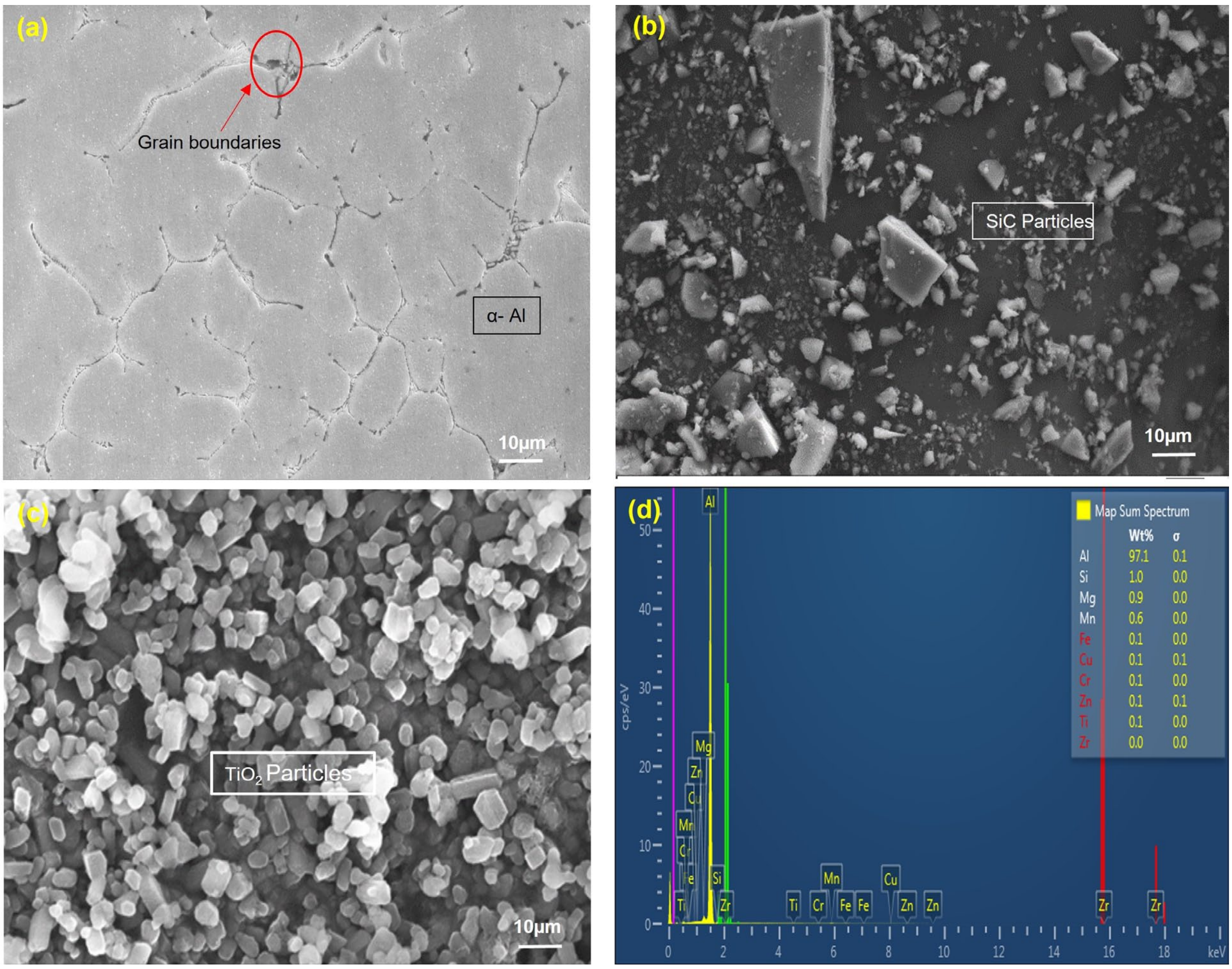

Fig. 1. (a) Microstructure of E-1, (b) Morphology of SiC particles, (c) Morphology of TiO_2 Particles, (d) EDX analysis of the E-1

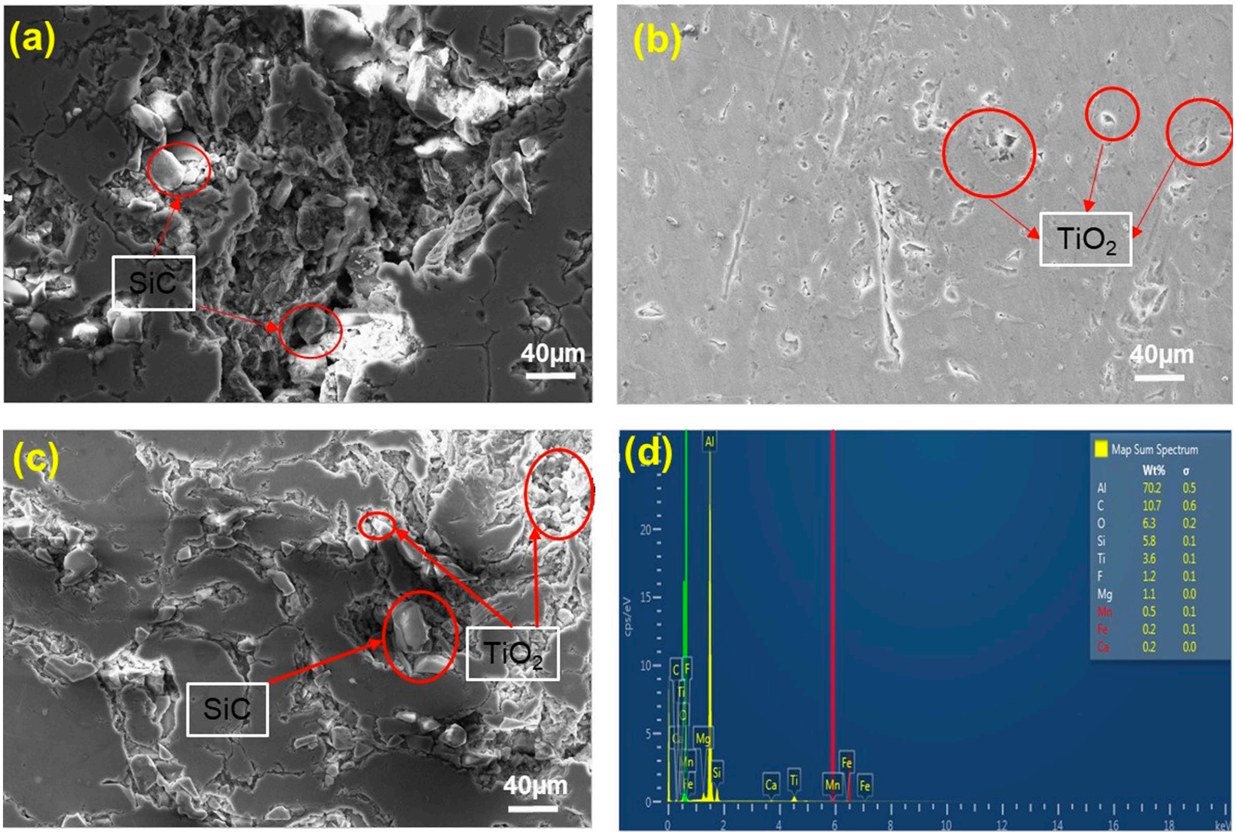

Fig. 2. Microstructure of (a) E-2, (b) E-3, (c) E-4, (d) EDX analysis of E-4

spots. The composites exhibited uniform distribution of reinforcements with minimal voids and discontinuities, which helps in an excellent interfacial bonding between metal matrix material and reinforcements.

3.2. Phase analysis

The phase analysis of samples for various materials (E-1, E-2, E-3, and E-4) was done by XRD technique, and the results are shown in Fig. 3. The phase analysis outcomes validate the occurrence of SiC and TiO_2 particles in the Al matrix. The sharp diffraction peaks of Al were at the 2θ angles of 38.6°(111), 44.8° (200), 65.2°(220), and 78.3° (311), very weak peaks of SiC were at the 2θ angles of 35.7° (111) and 60.2° (220) and TiO_2 peaks were at the 2θ angle of 48.2° (004). The XRD results confirm that there were no other peaks or impurities present. A small portion of reinforcements was hard to identify in the XRD spectrum. In contrast, the intensity of these peaks enhanced with increasing the weight percentage of reinforcement [46].

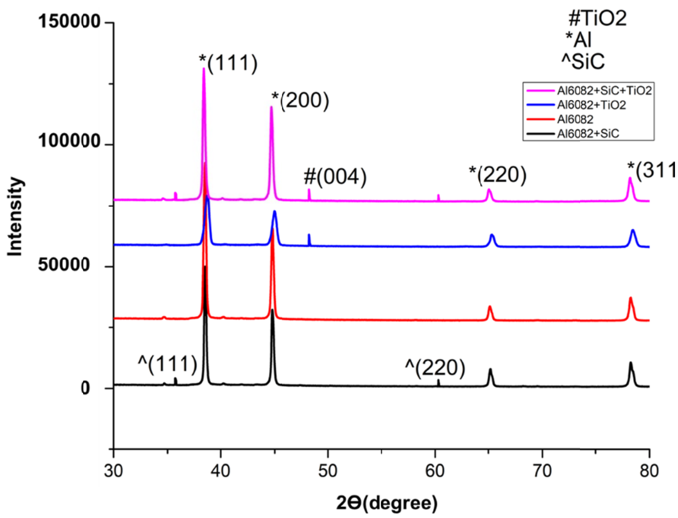

Fig. 3. XRD analysis of different conditions

3.3. Tensile test and hardness

Fig. 4 depicts the tensile strength and hardness of samples for different materials (E-1, E-2, E-3, and E-4). The experimental results show that E-4 samples exhibit more strength and hardness than the other samples. The hybrid composite's maximum hardness and strength were observed at 83 BHN and 205 MPa, respectively. The hardness and tensile strength of the hybrid composite were increased by 12.5%, 6.4%, and 22% and12.6%, 6.5%, and 32.5% to Al6082-SiC composite, Al6082-TiO_2 composite, and matrix alloy, respectively. This occurred due to the addition of reinforcements (SiC and TiO_2) to the aluminium metal matrix, provided high resistance to plastic deformation, encouraged the increase in the high hardness and tensile strength of the hybrid composite, and increased the load-bearing ability of the hybrid composite. The reinforcement addition also increases the strength and hardness of the single reinforced composites compared to the unreinforced aluminium matrix alloys. For apparent differences, the corresponding mechanical data are shown in TABLE 3.

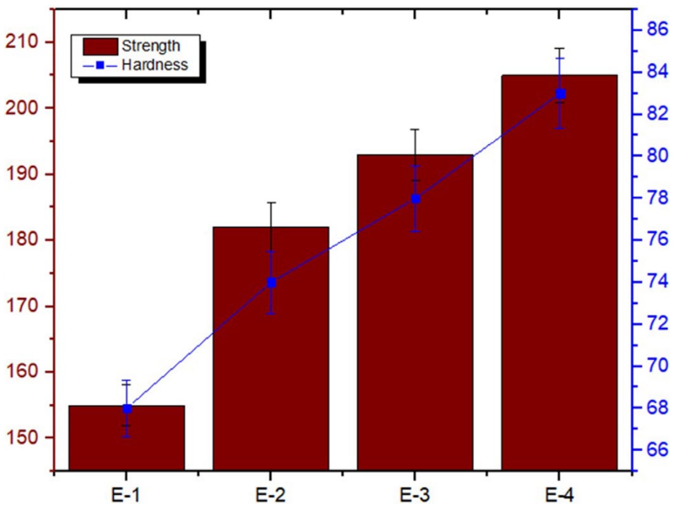

Fig. 4. Strength and hardness of the materials

It was observed that enhanced strength was due to the dispersion hardening effect, the load transfer mechanism, and or own strengthening mechanisms [47]. However, the ductility of reinforced samples was decreased due to the formation of voids and nucleation in the matrix around reinforcement materials [48]. The elongation of the hybrid composite was reduced by 7.5%, 2.5%, and 36.5% to Al6082-SiC composite, Al6082-TiO_2 composite and matrix alloy, respectively. One of the accepted strengthening mechanisms is the load transfer mechanism which occurs due to transmit of load (Eq. (1)) from matrix material to the solid particles of reinforcements through their interface [46].

$$\Delta\sigma\text{load} = 0.5\, f\sigma m \tag{1}$$

Where f = fractional volume of reinforcements σm = yield strength of the matrix alloy in (MPa).

TABLE 3

Ultimate tensile strength (UTS) and hardness values of different samples

Sample	UTS (MPa)	%Elongation	Hardness (BHN)
E-1	155	8.02	67
E-2	182	5.21	74
E-3	193	5.5	78
E-4	205	5.1	83

3.4. Impact test analysis

The Charpy impact test was performed for the materials (E-1, E-2, E-3, and E-4) at different sub-zero temperatures (room temperature, 0°C, –25°C, –50°C and –75°C), and results are shown in TABLE 4. Fig. 5 depicts that impact energy decreases at lower temperatures irrespective of the materials. It is because at lower temperatures brittleness nature of samples increases. In impact testing at all temperature conditions, impact energy increases with the addition of reinforcement SiC and TiO_2 particles to the matrix material (E-4), showing higher resistance to impact load when compared with other conditions (E-1, E-2, and E-3). The hybrid composite's highest impact energy was observed at room temperature. The maximum impact energy of hybrid composite (E-4) was 6.12 J which was increased by 11%, 10%, and 22.5% to Al6082-SiC composite, Al6082-TiO_2 composite, and matrix alloy, respectively, at room temperature. The decrease of impact strength with a reduction in temperature is an expected result as the ductility decreases with temperature [49].

TABLE 4

Impact energy in Joules at different temperatures

Condition	RT	0°C	–25°C	–50°C	–75°C
E-1	5.01	4.89	4.76	4.4	3.07
E-2	5.51	5.21	5.18	5.06	4.3
E-3	5.55	5.36	5.24	4.54	4.21
E-4	6.12	5.87	5.76	5.51	4.3

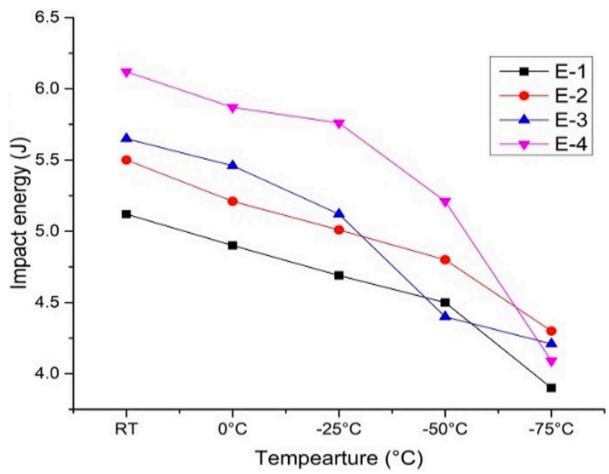

Fig. 5. Impact energy of the materials at different temperatures

3.5. Fractography analysis

3.5.1. Fracture surface of tensile samples

SEM images of fracture surfaces were taken for fractographic analyses, shown in Fig. 6. The fracture surface of the matrix alloy (E-1) was observed with dimples and cleavages; this confirms the ductile fracture. The fracture surfaces of E-2, E-3, and E-4 as shown in the Figs. 6(b-d), respectively. The changes in the behaviour of fracture surfaces of single-reinforced composites (E-2 and E-3) and hybrid composites (E-4) were observed. The fracture surfaces consist of dimple patterns and tear rigid, showing ductile and brittle fractures of mixed mode. The ductile fracture mechanism includes

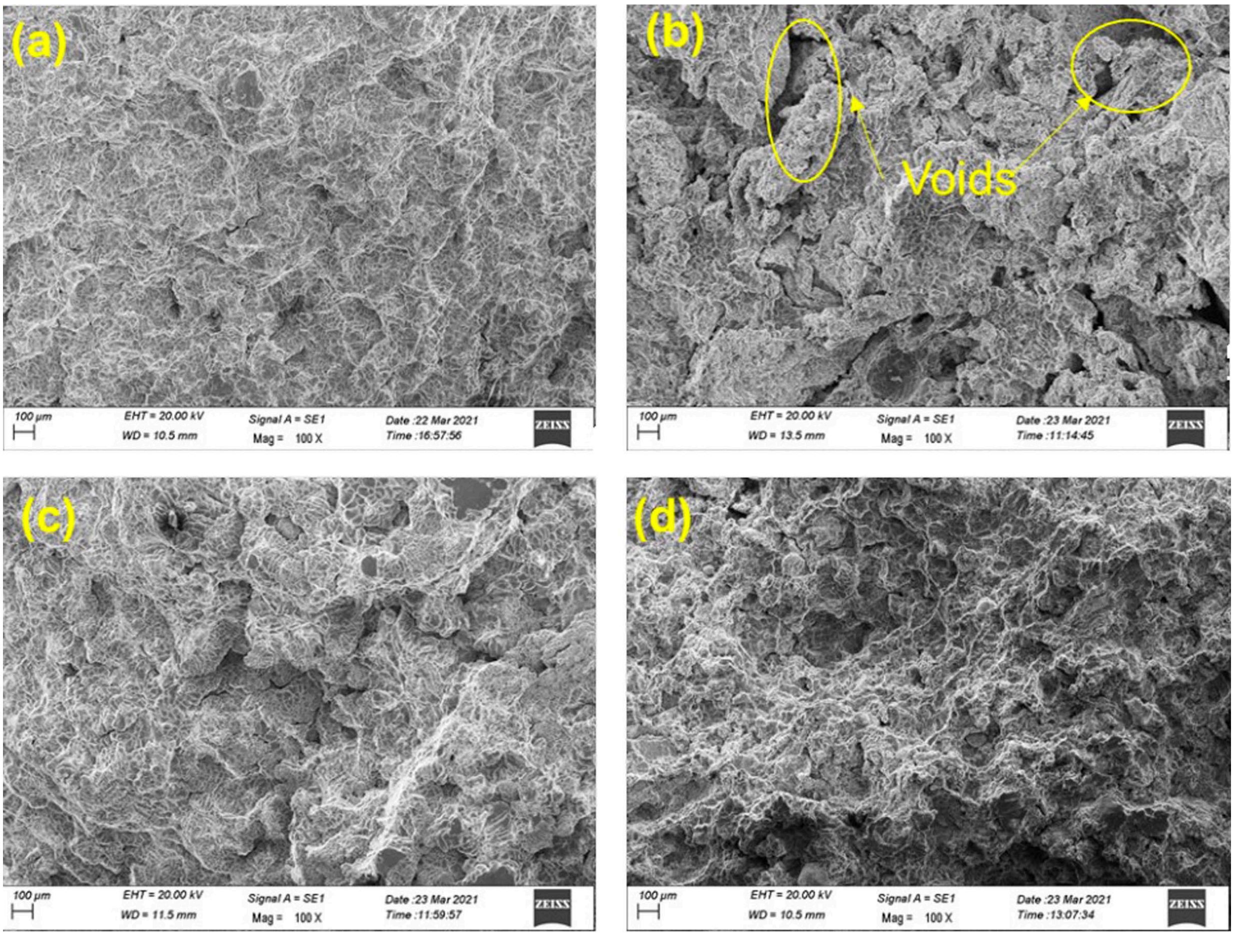

Fig. 6. The tensile fracture surfaces of (a) E-1, (b) E-2, (c) E-3, (d) E-4

nucleation, growth, and coalescence of voids in the matrix around reinforcement material. In contrast, brittle fracture in composites has features of particle pullout, crack growth, and crack propagation [49].

3.5.2. Fractography analysis of impact samples

The fracture surfaces of impact test samples for materials (E-1, E-2, E-3, and E-4) are shown in Fig. 7. The impact samples tested at room temperature depict a dimples structure. In contrast, samples at –75°C show the cleavage structure with microvoids and voids. The SEM images of fracture surfaces agree with the impact strengths obtained from testing.

3.6. Wear test analysis

Wear test was performed for materials (E-1, E-2, E-3 and E-4) at different high-temperature conditions (RT, 100°C, 175°C, 250°C and 325°C); after that wear results were analyzed. Figs. 8(a) and 8(b) show the variation in weight loss and the average coefficient of friction with different temperatures. Lower weight loss was observed in composite materials compared to Al6082 matrix alloys at different temperatures.

The hybrid composite exhibited excellent wear resistance to severe wear than the single reinforced composites at higher temperature regimes. The weight loss of all the materials was increased with an increase in temperature due to softening of materials. Weight loss of the E-2 composite was higher than the E-3 composite, up to 175°C and almost equal for both composites after 175°C. This is due to the precipitation (Mg_2Si) hardening of E-2 composites. The average friction coefficient of materials in different temperatures is shown in Fig. 8(b). At all temperatures, friction coefficients fluctuate about the mean level and decrease as the temperature increases. The friction coefficient fluctuations may be due to variations in contact between the sample and the disc [51]. The composites exhibited a lower frictional coefficient in comparison to the matrix alloy.

3.6.1. Analysis of wear surfaces

SEM was used to examine the wear surfaces after the wear test at room and high-temperature conditions. The morphological analysis of the wear surfaces shows that the wear debris obtained from the hybrid composite samples is fine and smooth, as shown in Fig. 9(d). The wear surfaces of matrix alloy (E-1) showed higher wear track marks and significantly wider grooves, as shown in Fig. 9(a). Over the sliding surface, a transfer layer of

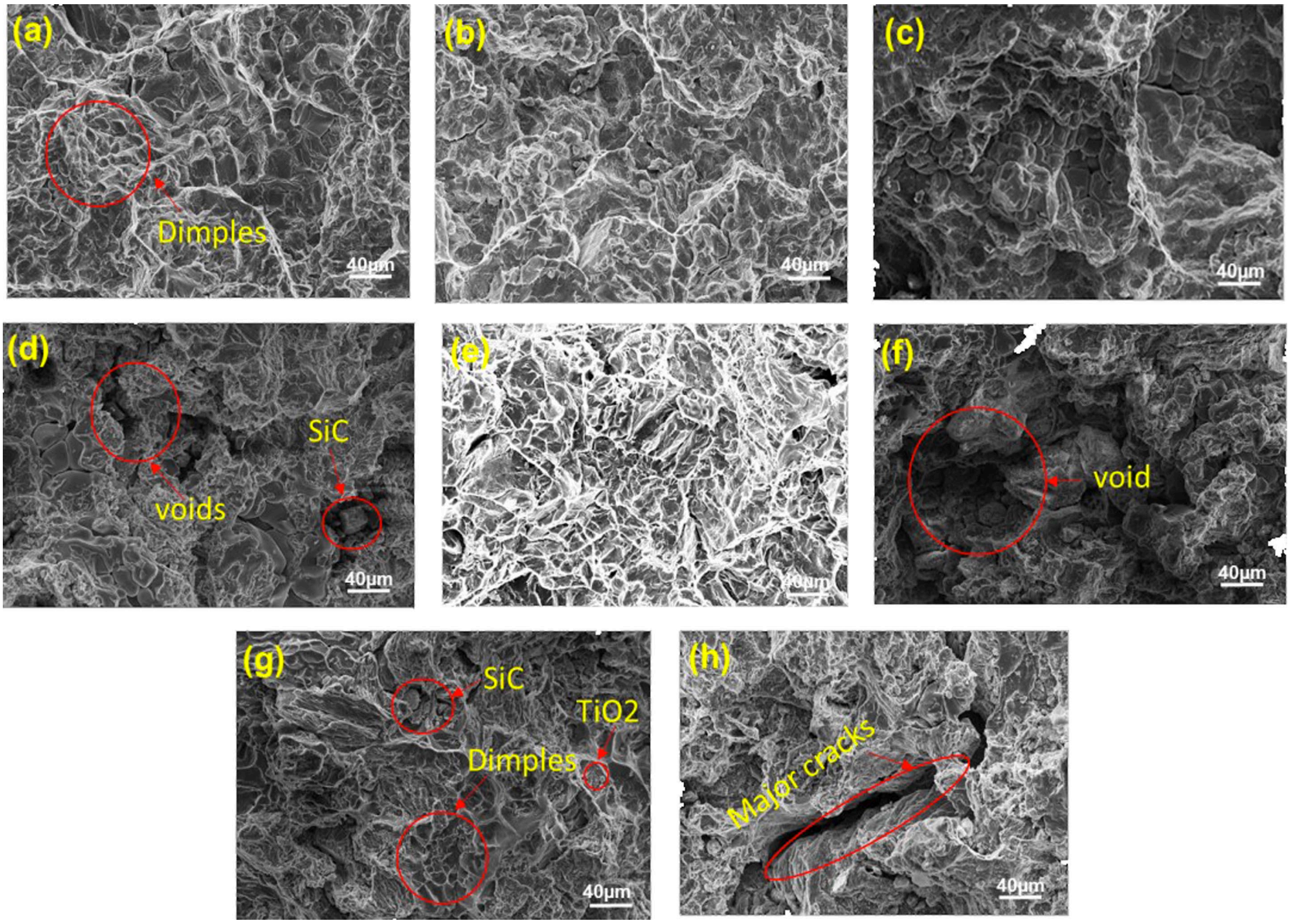

Fig. 7. Fractography of impact tests (a) matrix alloy at room temperature, (b) matrix alloy at –75°C, (c) E-2 at RT, (d) E-2 at –75°C, (e) E-3 at RT, (f) E-3 at –75°C, (g) E-4 at RT, (h) E-4 at –75°C

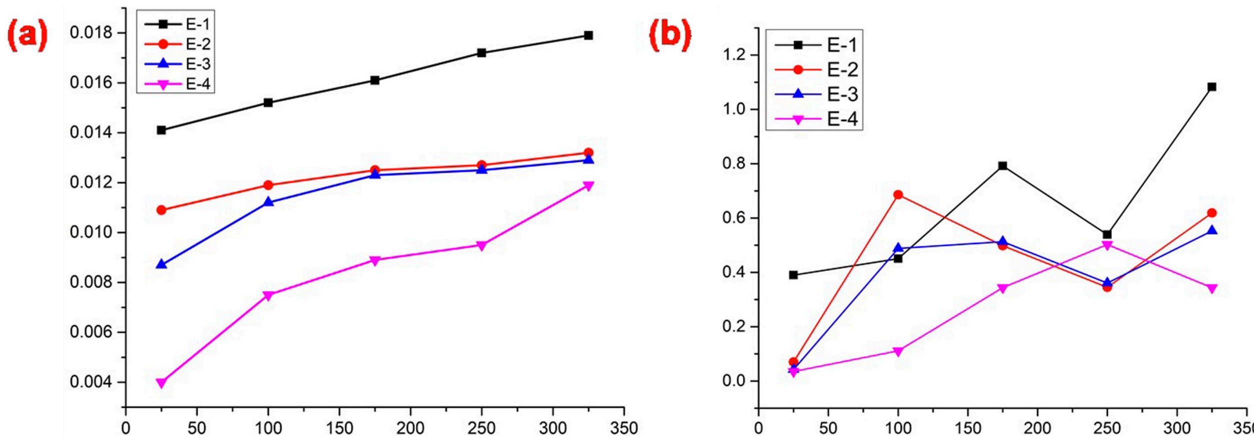

Fig. 8 (a) Weight loss of materials at different temperatures, (b) The friction coefficient of materials in different temperatures

compressed wear debris and wear tracks can be analysed. Before detaching, this layer reaches a specific thickness, which causes wear debris to form.

Comparatively, the cracks and wear debris in the Al6082-SiC composite (E-2) was less than that of the Al6082-TiO_2 composite (E-3), as shown in Figs. 9(b) and 9(c), due to the formation of precipitation at higher temperatures. Hybrid composite wear surfaces showed shallower grooves and minimum craters when collated with Al6082-SiC composite, Al6082-TiO_2 composite, and matrix alloy. Due to shallower grooves, the weight loss in composites is lower. Another factor contributing to composites' lower weight loss is their increased hardness compared to matrix alloys, which results in a smaller real contact area and, thus, a lower rate of wear [39].

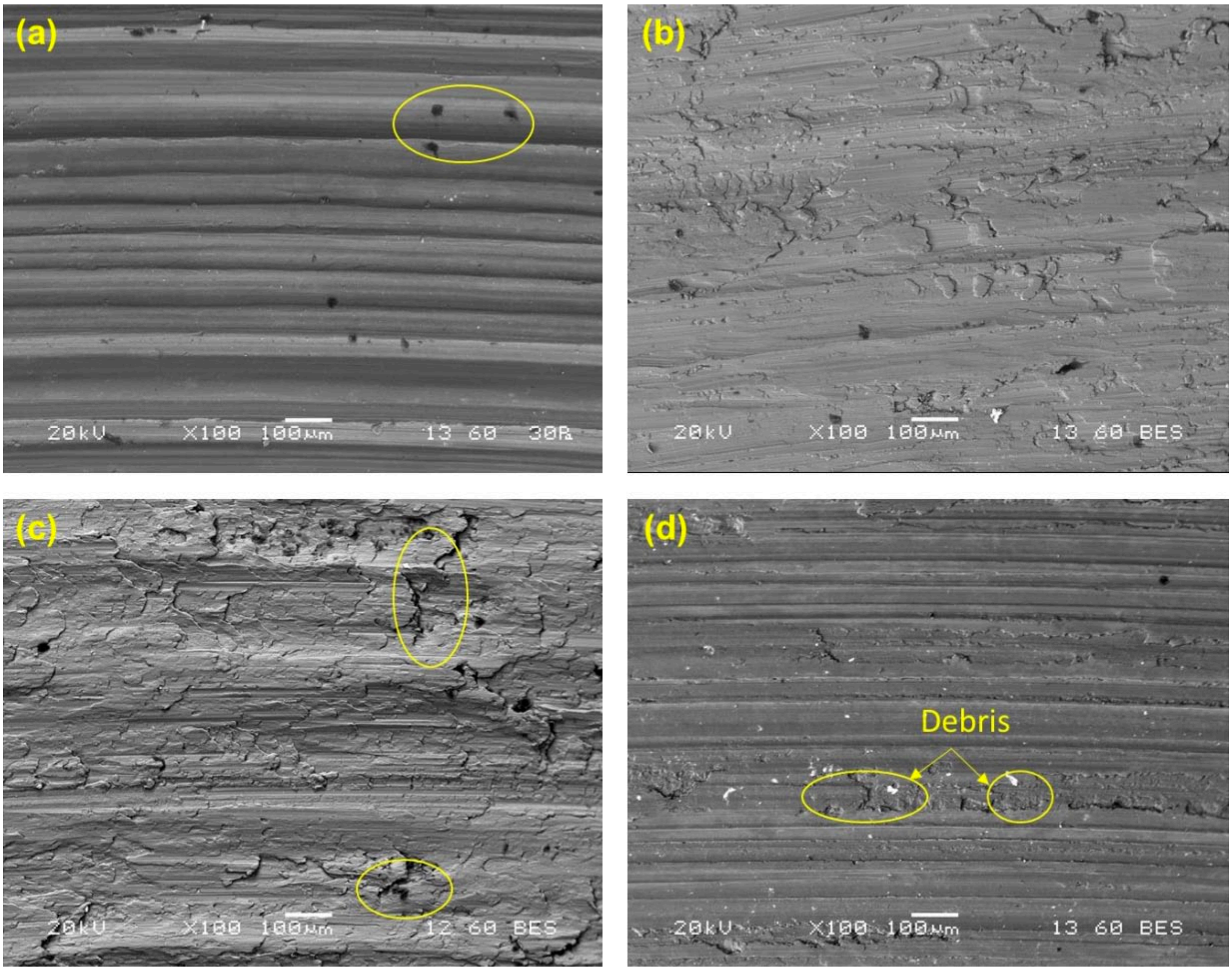

Fig. 9. The wear surfaces of (a) E-1, (b) E-2, (c) E-3, (d) E-4, at temperature of 250°C

4. Conclusions

The present study based on the microstructure, mechanical properties and high temperature sliding wear characterisation of Al6082-SiC-TiO_2 hybrid composite developed by stir casting process was investigated and distinguished to single reinforced composites (Al6082-SiC and Al6082-TiO_2) and matrix alloy. The outcomes of the researched study can be concluded as follows:

1. The microstructure of the single reinforced composites and hybrid composites revealed that the aluminium matrix consists of uniform distribution of reinforcement particles and minimal micro-voids and discontinuity.
2. The hybrid composites' hardness and ultimate tensile strength (UTS) showed higher hardness and tensile strength than matrix alloy and single-reinforced composites.
3. The impact energy decreased with decreasing temperatures, irrespective of the materials. The impact energy of hybrid composite was increased by 11%, 10%, and 22.5% to Al6082-SiC composite, Al6082-TiO_2 composite, and matrix alloy, respectively, at room temperature.
4. The fracture surfaces of both tensile and impact test samples exhibited cleavage fractures with minimum voids; it is evidence of a brittle fracture.
5. The hybrid composites have excellent wear resistance, irrespective of temperature, compared to the other materials.
6. The wear surfaces of hybrid composite showed shallower grooves compared to Al6082-SiC composite, Al6082-TiO_2 composite, and matrix alloy.

Hence, adding hard dispersoid particles in matrix materials increases the mechanical and tribological properties in different environmental temperatures. The hybrid composite shows superior properties to matrix alloy and single-reinforced composites.

Statements and declarations

This work was supported by AICTE and NPIU, a unit of the MHRD Government of India under the Collaborative Research Scheme (CRS) (CRS ID: 1-5728212525). The second author received a research fund from TEQIP-III.

REFERENCES

[1] W.S. Miller, L. Zhuang, J. Bottema, A.J. Wittebrood, P.D. Smet, A. Haszler, A. Vieregge, Recent development in aluminium alloys

for the automotive industry, Mater. Sci. Eng. A **280** (1), 37-49 (2000). DOI: https://doi.org/10.1016/S0921-5093(99)00653-X

[2] K.R. Brown, M.S. Venie, R.A. Woods, The increasing use of aluminium in automotive applications, JOM **47** (7), 20-23 (1995). DOI: https://doi.org/10.1007/BF03221224

[3] R.K. Singh, A. Telang, S. Das, Microstructure, mechanical properties and two-body abrasive wear behavior of hypereutectic Al−Si−SiC composite, T. Nonferr. Metal. Soc. **30** (1), 65-75 (2020). DOI: https://doi.org/10.1016/S1003-6326(19)65180-0

[4] J. Xu, G. Chen, Z. Zhang, Y. Zhao, T. Zhang, C. Zhang, D. Dali, Effect of Al-3 wt% Al2O3 master alloy fabricated by calcined kaolin on grain refinement and mechanical properties of A356 alloy, J. Alloys Compd. **862,** 158512 (2021). DOI: https://doi.org/10.1016/j.jallcom.2020.158512

[5] M. Hashemi, R. Jamaati, M.R. Toroghinejad, Microstructure and mechanical properties of Al/SiO2 composite produced by CAR process, Mater. Sci. Eng. A **532**, 275-281 (2012). DOI: https://doi.org/10.1016/j.msea.2011.10.091

[6] L. Lukose, K. Babu, S.A. Srinivasan, Development of Aluminium 6082 alloy reinforced with Al2O3 by die casting and investigation of microstructural and mechanical properties, Mater. Today: Proc. **27** (3), 2520-2525 (2020). DOI: https://doi.org/10.1016/j.matpr.2019.09.229

[7] P.K. Yadav, G. Dixit, B. Kuriachen, M.K. Verma, S.K. Patel, R.K. Singh, Effect of reinforcements and abrasive size on high-stress tribological behaviour of aluminium piston matrix composites, J. Bio- Tribo-Corros. **6** (1), 1-14 (2021). DOI: https://doi.org/10.1007/s40735-019-0317-6

[8] B. P. Nagasai, C.H. Anusha, A. Rajesh, Study on mechanical properties of Al-6061/ZrO2 reinforced metal matrix composites, Mater. Today: Proc. **47** (14), 4552-4557 (2021). DOI: https://doi.org/10.1016/j.matpr.2021.05.424

[9] A.K. Singh, S. Soni, R.S. Rana, Microstructure evolution, mechanical behavior and fracture analysis of ultrasonic-assisted stir-squeeze cast high strength AA7068/ZrO2p/Grp composite under thermal aging, Part. Sci. Technol. **40** (4), 445-464 (2021). DOI: https://doi.org/10.1080/02726351.2021.1958398

[10] D.J. Lloyd, Particle reinforced aluminium and magnesium matrix composites, Int. Mater. Rev. **39** (1), 1-23 (1994). DOI: https://doi.org/10.1179/imr.1994.39.1.1

[11] P.K. Rohatgi, Cast aluminium-matrix composites for automotive applications, JOM. **43**, 10-15 (1991). DOI: https://doi.org/10.1007/BF03220538

[12] R.F. Guo, N. Guo, P. Shen, L.K. Yang, Q.C. Jiang, Effects of ceramic lamellae compactness and interfacial reaction on the mechanical properties of nacre-inspired Al/Al2O3−ZrO2 composites, Mater. Sci. Eng. A **718**, 326-334 (2018). DOI: https://doi.org/10.1016/j.msea.2018.01.088

[13] N.Ch. Kaushik, R.N. Rao, Influence of applied load on abrasive wear depth of hybrid Gr/SiC/Al-Mg-Si composites in two body condition, J. Tribol. **139** (6), 061601 (2017). DOI: https://doi.org/10.1115/1.4035779

[14] S. Doddapanen, S. Sharma, M.C.G. Shankar, M. Shettar, A. Hegde, Effect of precipitation hardening treatment on hardness and tensile behaviour of stir cast LM4 hybrid composites through TEM and fractography analysis, J. Mater. Res. Technol. **23**, 1584-1598 (2023). DOI: https://doi.org/10.1016/j.jmrt.2023.01.127

[15] Q. Hu, H. Zhao, J. Ge, Microstructure and mechanical properties of (B4C+Al3Ti)/Al Hybrid composites fabricated by a two-step stir casting process, Mater. Sci. Eng. A. **650**, 478-482 (2015). DOI: https://doi.org/10.1016/j.msea.2015.10.041

[16] A. Ahmadi, M.R. Toroghinejad, A. Najafizadeh, Evaluation of microstructure and mechanical properties of Al/Al2O3/SiC hybrid composite fabricated by accumulative roll bonding process, Mater. Des. **53**, 13-19 (2014). DOI: https://doi.org/10.1016/j.matdes.2013.06.064

[17] S. Rangrej, S. Pandya, J. Menghani, Effects of reinforcement additions on properties of aluminium matrix composites – A review, Mater. Today: Proc. **44**, 637-641 (2021). DOI: https://doi.org/10.1016/j.matpr.2020.10.604

[18] D.F. Hasson, S.M. Hoover, C.R. Crowe, Effect of thermal treatment on the mechanical and toughness properties of extruded SiCw/aluminium 6061 metal matrix composite, J. Mater. Sci. **20**, 4147-54 (1985). DOI: https://doi.org/10.1007/BF00552410

[19] C.M. Friend, Toughness in metal matrix composites, Mater. Sci. Technol. **5**, 1-7 (1989). DOI: https://doi.org/10.1179/mst.1989.5.1.1

[20] V.C. Nardone, J.R. Strife, K.M. Prewo, Microstructurally toughened particulate-reinforced aluminum matrix composites, Metall. Mater. Trans. A. **22**, 171-82 (1991). DOI: https://doi.org/10.1007/BF03350959

[21] J.P. Unsworth, S. Bandyopadhyay, Effect of thermal ageing on hardness, tensile and Impact properties of an alumina microsphere reinforced aluminium metal–matrix composite, J. Mater. Sci. **29**, 4645-50 (1994). DOI: https://doi.org/10.1007/BF00376291

[22] H. Ahlatci, E. Candan, H. Çimenoğlu, Effect of particle size on the mechanical properties of 60 vol.% SiCp reinforced Al matrix composites, Int. J. Mater. Res. **93** (4), 330-333 (2002).

[23] P. Das, R. Jayaganthan, I.V. Singh, Tensile and impact-toughness behavior of cryorolled Al 7075 alloy, Mater. Des. **32** (3), 1298-1305 (2011). DOI: https://doi.org/10.1016/j.matdes.2010.09.026

[24] P.K. Yadav, S.K. Patel, V.P. Singh, M.K. Verma, R.K. Singh, B. Kuriachen, G. Dixit, Effect of Different Reinforced Metal-Matrix Composites on Mechanical and Fracture Behaviour of Aluminium Piston Alloy, J. Bio- Tribo- Corros. **7** (2), 54 (2021). DOI: https://doi.org/10.1007/s40735-021-00478-8

[25] S. Ozden, R. Ekici, F. Nair, Investigation of impact behaviour of aluminium based SiC particle reinforced metal–matrix composites, Compos. Part A Appl. **38**, 484-494 (2007). DOI: https://doi.org/10.1016/j.compositesa.2006.02.026

[26] T. Zeuner, P. Stojanov, P.R. Sahm, H. Ruppert, A. Engels, Developing trend in disc brake technology for rail application, Mater. Sci. Technol. **14**, 857-863 (1998). DOI: https://doi.org/10.1179/mst.1998.14.9-10.857

[27] S. Das, Development of aluminium alloy composites for engineering applications, Trans. Indian Inst. Met. **57** (4), 325-325 (2004).

[28] M.K. Surappa, Aluminium matrix composites challenges and Opportunities, Sadhana-Acad. P. Eng. S. **28** (1-2), 319-334 (2003). DOI: https://doi.org/10.1007/BF02717141

[29] S. Das, D.P. Mondal, O.P. Modi, R. Dasgupta, Influence of experimental parameters on the erosive–corrosive wear of Al–SiC particle composite, Wear **231** (2), 195-205 (1999).
DOI: https://doi.org/10.1016/S0043-1648 (99)00106-4

[30] S.V. Prasad, R. Asthana, Aluminum Metal-Matrix Composites for Automotive applications: Tribology Considerations, Tribol. Lett. **17**, 445-453 (2004).
DOI: https://doi.org/10.1023/B:tril.0000044492.91991.f3

[31] H. Ahlatci. H. Çimenoğlu. E. Candan, Mechanical properties of Al-60Pct SiCp composites alloyed with Mg Metall, Mater. Trans. A **35**, 2127-2141 (2004).
DOI: https://doi.org/10.1007/s11661-004-0161-1

[32] N. Muralidharan, K. Chockalingam, I. Dinaharan, K. Kalaiselvan, Microstructure and mechanical behavior of AA2024 aluminum matrix composites reinforced with in situ synthesised ZrB2 particles, J. Alloys Compd. **735**, 2167-2174 (2018).
DOI: https://doi.org/10.1016/j.jallcom.2017.11.371

[33] M. Roy, B. Venkataraman, V. Bhanuprasad, Y. Mahajan, G. Sundararajan, The Effect of Particulate Reinforcement on the Sliding Wear Behavior of Aluminum Matrix Composites, Metall. Mater. Trans. A **23**, 2833-2847 (1992).
DOI: https://doi.org/10.1007/BF02651761

[34] Y. Sahin, Wear behaviour of aluminium alloy and its composites reinforced by SiC particles using statistical analysis, Mater. Des. **24**, 95-103 (2003).
DOI: https://doi.org/10.1016/S0261-3069(02)00143-7

[35] Y. Sahin, Optimisation of testing parameters on the wear behaviour of metal matrix composites based on the Taguchi method, Mater. Sci. Eng. A **408** (1-2), 1-8 (2005).
DOI: https://doi.org/10.1016/j.msea.2004.11.012

[36] Y. Sahin, Abrasive wear behaviour of SiC/2014 aluminium composite, Tribol. Int. **43** (5-6), 939-943 (2010).
DOI: https://doi.org/10.1016/j.triboint.2009.12.056

[37] D.P. Mondal, S. Das, High stress abrasive wear behaviour of aluminium hard particle composites: Effect of experimental parameters, particle size and volume fraction, Tribol. Int. **39** (6), 470-478 (2006). DOI: https://doi.org/10.1016/j.triboint.2005.03.003

[38] R. Sharma, Anesh, D.K. Dwivedi, Solutionising temperature and abrasive wear behavior of cast Al–Si–Mg alloys, Mater. Des. **28** (6), 1975-1981 (2007).
DOI: https://doi.org/10.1016/j.matdes.2006.04.011

[39] K.B. Shah, S. Kumar, D.K. Dwivedi, Aging temperature and abrasive wear behavior of cast Al– (4%, 12%, 20%)Si–0.3% Mg alloys, Mater. Des. **28** (6), 1968-1974 (2007).
DOI: https://doi.org/10.1016/j.matdes.2006.04.012

[40] R.K. Singh, A. Telang, M.M. Khan, Effect of T6 heat treatment on microstructure, mechanical properties and abrasive wear response of Fly Ash reinforced Al-Si alloy, Mater. Today: Proc. **4** (9), 10062-10068 (2017).
DOI: https://doi.org/10.1016/j.matpr.2017.06.321

[41] R.K. Singh, A. Telang, S. Das, Microstructure, mechanical, and high-stress abrasive wear behaviour of as-cast and heat-treated Al–Si–SiCp composite, Int. J. of Mater. Res. **110** (2), 121-129 (2019). DOI: https://doi.org/10.3139/146.111727

[42] R.K. Singh, A. Telang, S. Das, The influence of abrasive size and applied load on abrasive wear of Al-Si–SiCp composite, Arab. J. Sci. Eng. **47**, 8617-8628 (2022).
DOI: https://doi.org/10.1007/s13369-021-06349-1

[43] A.K. Singh, S. Soni, R.S. Rana, sliding wear response of ultrasonic-assisted stir-squeeze cast Al-Zn (-Mg) alloy/ZrO2p composite Wear mechanism and subsurface deformation, Surf. Topogr. **10**, 025020 (2022).
DOI: https://doi.org/10.1088/2051-672X/ac6f71

[44] A.K. Singh, S. Soni, R.S. Rana, Wear Mechanism Maps for Stir-Squeeze Cast AA7068 Alloy/ZrO2p Composite in Accordance with Normal Load Versus Sliding Speed Diagram, Trans. Indian Inst. Met. **75**, 2867-2874 (2022).
DOI: https://doi.org/10.1007/s12666-022-02662-x

[45] A.K. Singh, S. Soni, R.S. Rana, Mechanical and sliding wear behavior of stir-squeeze cast and T6 heat-treated AA7068-ZrO2p composite, Compos. Interfaces 1-27 (2022).
DOI: https://doi.org/10.1080/09276440.2022.2120736

[46] M. Singla, L. Singh, V. Chawla, Study of Wear Properties of Al-SiC Composites, J. Miner. Mater. Charact. Eng. **8** (10), 813-821 (2009). DOI: https://doi.org/10.4236/jmmce.2009.810070

[47] M.O. Bodunrin, K.K. Alaneme, L.H. Chown, Aluminium matrix hybrid composites: a review of reinforcement philosophies; mechanical, corrosion and tribological characteristics, J. Mater. Res. Technol. **4** (4), 434-445 (2015).
DOI: https://doi.org/10.1016/j.jmrt.2015.05.003

[48] S. Ozden, S, Ekici F.Nair, Investigation of impact behaviour of aluminium based SiC particle reinforced metal–matrix composites, Compos. Part A Appl. Sci. Manuf. **38** (2), 484-494 (2007).
DOI: https://doi.org/10.1016/j.compositesa.2006.02.026

[49] M. Suhandani, P. Poppy, J.A. Razak, Impact, Hardness and Fracture Morphology of Aluminium Alloy (Al-Si) filled Cobalt Oxide Nanoparticles at Various Stir Casting Temperatures, Malays. J. Compos. Sci. Manuf. **5** (1), 11-20 (2021).
DOI: https://doi.org/10.37934/mjcsm.5.1.1120

[50] B.N. Sarada, P.L.S. Murthy, G. Ugrasen, Hardness and Wear Characteristics of Hybrid Aluminium Metal Matrix Composites Produced by Stir Casting Technique, Mater. Today: Proc. **2** (4-5), 2878-2885 (2015).
DOI: https://doi.org/10.1016/j.matpr.2015.07.305

[51] A. Pramanik, Effects of reinforcement on wear resistance of aluminum matrix composites, T. Nonferr. Metal. Soc. **26** (2), 348-358 (2016). DOI: https://doi.org/10.1016/S1003-6326(16)64125-0